

Cite as: Y. Sivan *et al.*, *Science*  
10.1126/science.aaw9367 (2019).

# Comment on “Quantifying hot carrier and thermal contributions in plasmonic photocatalysis”

Yonatan Sivan<sup>1,2\*</sup>, Joshua Baraban<sup>3\*</sup>, Ieng Wai Un<sup>1,4\*</sup>, Yonatan Dubi<sup>2,3\*†</sup>

<sup>1</sup>Unit of Electro-Optics Engineering, Ben-Gurion University of the Negev, Beer-Sheva, Israel. <sup>2</sup>Ilse Katz Center for Nanoscale Science and Technology, Ben-Gurion University of the Negev, Beer-Sheva, Israel. <sup>3</sup>Department of Chemistry, Ben-Gurion University of the Negev, Beer-Sheva, Israel. <sup>4</sup>Joan and Irwin Jacobs TIX Institute, National Tsing Hua University, Hsinchu City, Taiwan.

\*These authors contributed equally to this work.

†Corresponding author. Email: jdubi@bgu.ac.il

Zhou *et al.* (Reports, 5 October 2018, p. 69) claim to have proven dominance of “hot” electrons over thermal effects in plasmonic photocatalysis. We identify experimental flaws that caused overestimation of the hot carrier contribution. As an alternative interpretation, we fully reproduce their data using a purely thermal Arrhenius law with a fixed activation energy and intensity-dependent heating.

Recently, Zhou *et al.* (1) reported quantification of the contributions of nonthermal (“hot”) carriers versus thermal effects in plasmon-mediated photocatalytic ammonia decomposition. The authors placed Cu-Ru nanoparticles within a 300- $\mu\text{m}$ -thick layer of MgO and subjected this catalyst pellet to pulsed illumination. They monitored the pellet surface temperature  $T_s$  (using a thermal imaging camera) and the  $\text{H}_2$  production rate  $R$  as a function of illumination intensity and wavelength, and fitted the  $\text{H}_2$  production rate with an Arrhenius activation function,

$$R = R_0 \exp\left[-\frac{E_a(I_{\text{inc}}, \lambda)}{k_B T(I_{\text{inc}}, \lambda)}\right] \quad (1)$$

where  $E_a(I_{\text{inc}}, \lambda)$  is an empirically determined intensity- and wavelength-dependent activation energy, and  $R_0$  is a constant that depends on the exact details of the sample and reaction. These simultaneous measurements were used to extract the dependence of the activation energy on the illumination intensity and wavelength, phenomena whose origins are theoretically unknown. Furthermore, by performing a control experiment in the dark (thermocatalysis) at the previously measured temperatures, Zhou *et al.* show that the contribution of the “hot” electrons to the reaction is much greater than the contribution of purely thermal effects. Notably, the authors did not fit their data with any theory, such that the results remain empirical and specific to the sample studied.

Unfortunately, it is apparent from the supplementary materials of (1) that their measured temperatures are un-

likely to be accurate. Figure S11 of (1) shows that the default thermal camera settings were used, which are wholly inappropriate here. Of primary concern is the emissivity, set by default to 0.95 but likely to be no more than 0.5 in the most optimistic scenario, based on the emissivity literature for Cu (2), Ru (3),  $\text{Al}_2\text{O}_3$  (4), and MgO (5). Even a value of 0.02 is not out of the question, but we estimate 0.2 on the basis of the material composition reported in (1). The exact sample emissivity depends critically for any given material on temperature, wavelength range, morphology, and direction (6); suffice it to say that there is no practical substitute for empirical calibration, and therefore the temperatures measured in (1) almost certainly contain systematic errors.

Crucially, such an error would inevitably lead to a measured temperature lower than the true temperature. Based on the Stefan-Boltzmann law, the measured surface temperature is at least ~20% lower than the actual temperature and is highly likely to be substantially lower. For the ~1.27 eV activation energies measured in the dark in (1), the exponential sensitivity of the reaction rate means that such an error in the temperature causes an underestimate of at least three orders of magnitude in the thermocatalysis reaction rate at room temperature; a more accurate treatment of the scaling of the radiance with temperature that accounts for the limited spectral bandwidth actually detected by the thermal camera by integrating over the 8- to 14- $\mu\text{m}$  band yields an even larger error (7).

Additional doubts regarding the accuracy of the temperature readings in (1) arise from insufficient spatial resolution and possible improper focusing of the camera. However, more critical is the neglect of temperature non-

niformities along the pellet depth (8, 9). These cause the thermal contribution in the photocatalysis experiment to be different from the thermal contribution in the dark control, such that the differences of the latter from the photocatalysis rate are incorrectly interpreted as “hot” electron action. More generally, the thermocatalysis control experiment is inappropriate in practice, because the thermal camera measures the average temperature throughout the sample, whereas catalytic rates are exponentially sensitive to temperature variations and thus “measure” an exponential average (9). For the conditions of (I), the exponential sensitivity of the reaction on the temperature causes even a 1% change in the temperature (due to inhomogeneities in space) to result in a reaction rate change of several tens of percent.

In light of the above, we note that the data of (I) and other related works can be straightforwardly reproduced using a conventional thermal model with minimal fit parameters. Figure 1 shows that an excellent fit to all the curves of figure 2 in (I) is obtained by assuming that the reaction rate still obeys an Arrhenius form with an intensity-independent activation energy, and that the effective reactor temperature grows linearly with the incident illumination (I0, II),

$$R = R_0 \exp \left[ -\frac{E_a}{k_B T(I_{\text{inc}}, \lambda)} \right] \quad (2)$$

$$T(I_{\text{inc}}, \lambda) = T_s + a(\lambda) I_{\text{inc}} \quad (3)$$

where  $T$  is the effective temperature of the reactor,  $T_s$  is the surface temperature measured in (I), and  $I_{\text{inc}}$  is the average incident intensity.

The coefficient  $a$  can be deduced by fitting just one set of data points, corresponding to one value of intensity (e.g., squares in Fig. 1). We thereby find the value  $a \sim 180 \text{ K/W cm}^{-2}$ . With  $E_a$  and  $a$  now known, the rest of the data points in Fig. 1 (for different intensities, i.e., green triangles, diamonds, and circles) can be reproduced with no additional parameters.

This value of  $a$  predicts that for the reported data at an average intensity of  $3.2 \text{ W/cm}^2$  [figure 2A in (I)], the effective temperature of the reactor is  $\sim 1150 \text{ K}$ , roughly twice that measured by the authors ( $\sim 566 \text{ K}$ ); this is in accordance with the inappropriately high emissivity used in (I), as described above. Furthermore, the independent calculation predicts a significant temperature gradient across the depth of the sample, thus confirming the inadequacy of the control thermocatalysis experiment. This fact, together with the calculated weak sensitivity to the particle properties and

density, allows us to conclude that potential particle melting may affect the overall reaction rate only mildly. [See also the Faraday Discussion meeting protocol associated with (I2).]

The simplicity of the above argument (and the extraordinary fit it provides to the data) implies that, if only by virtue of Ockham’s razor, a thermal mechanism is far more likely to be responsible for the reaction rates measured in (I). We believe that conclusive experimental differentiation between thermal and nonthermal effects will have better prospects with thinner pellets, or ultimately in single-particle studies (I3, I4).

## REFERENCES

1. L. Zhou, D. F. Swearer, C. Zhang, H. Robotjazi, H. Zhao, L. Henderson, L. Dong, P. Christopher, E. A. Carter, P. Nordlander, N. J. Halas, Quantifying hot carrier and thermal contributions in plasmonic photocatalysis. *Science* **362**, 69–72 (2018). doi:10.1126/science.aat6967 Medline
2. I. Setién-Fernández, T. Echániz, L. González-Fernández, R. B. Pérez-Sáez, M. J. Tello, Spectral emissivity of copper and nickel in the mid-infrared range between 250 and 900°C. *Int. J. Heat Mass Transfer* **71**, 549–554 (2014). doi:10.1016/j.ijheatmasstransfer.2013.12.063
3. N. Milošević, I. Nikolić, Thermophysical properties of solid phase ruthenium measured by the pulse calorimetry technique over a wide temperature range. *Int. J. Mater. Res.* **106**, 361–367 (2015). doi:10.3139/146.111192
4. D. T. Vader, R. Viskanta, F. P. Incropera, Design and testing of a high-temperature emissometer for porous and particulate dielectrics. *Rev. Sci. Instrum.* **57**, 87–93 (1986). doi:10.1063/1.1139125
5. A. M. Hofmeister, E. Keppel, A. K. Speck, Absorption and reflection infrared spectra of MgO and other diatomic compounds. *Mon. Not. R. Astron. Soc.* **345**, 16–38 (2003). doi:10.1046/j.1365-8711.2003.06899.x
6. R. Siegel, J. R. Howell, *Thermal Radiation Heat Transfer: The Blackbody, Electromagnetic Theory, and Material Properties* (Scientific and Technical Information Division, NASA, 1968).
7. W. K. Widger Jr., M. P. Woodall, Integration of the Planck Blackbody Radiation Function. *Bull. Am. Meteorol. Soc.* **57**, 1217–1219 (1976). doi:10.1175/1520-0477(1976)057<1217:OTPBR>2.0.CO;2
8. H. Li, M. Rivallan, F. Thibault-Starzyk, A. Travert, F. C. Meunier, Effective bulk and surface temperatures of the catalyst bed of FT-IR cells used for in situ and operando studies. *Phys. Chem. Chem. Phys.* **15**, 7321–7327 (2013). doi:10.1039/c3cp50442e Medline
9. X. Zhang, X. Li, M. E. Reish, D. Zhang, N. Q. Su, Y. Gutiérrez, F. Moreno, W. Yang, H. O. Everitt, J. Liu, Plasmon-enhanced catalysis: Distinguishing thermal and nonthermal effects. *Nano Lett.* **18**, 1714–1723 (2018). doi:10.1021/acs.nanolett.7b04776 Medline
10. G. Baffou, R. Quidant, Thermo-plasmonics: Using metallic nanostructures as nano-sources of heat. *Laser Photonics Rev.* **7**, 171–187 (2013). doi:10.1002/lpor.201200003
11. G. Baffou, H. Rigneault, Femtosecond-pulsed optical heating of gold nanoparticles. *Phys. Rev. B* **84**, 035415 (2011). doi:10.1103/PhysRevB.84.035415
12. Y. Sivan, I. W. Un, Y. Dubi, Assistance of metal nanoparticles in photocatalysis – nothing more than a classical heat source. *Faraday Discuss.* **10.1039/C8FD00147B** (2019). doi:10.1039/C8FD00147B
13. C.-Y. Wu, W. J. Wolf, Y. Levartovsky, H. A. Bechtel, M. C. Martin, F. D. Toste, E. Gross, High-spatial-resolution mapping of catalytic reactions on single particles. *Nature* **541**, 511–515 (2017). doi:10.1038/nature20795 Medline
14. E. Cortés, W. Xie, J. Cambiasso, A. S. Jermyn, R. Sundararaman, P. Narang, S.

7 February 2019; accepted 17 April 2019  
Published online 3 May 2019  
10.1126/science.aaw9367

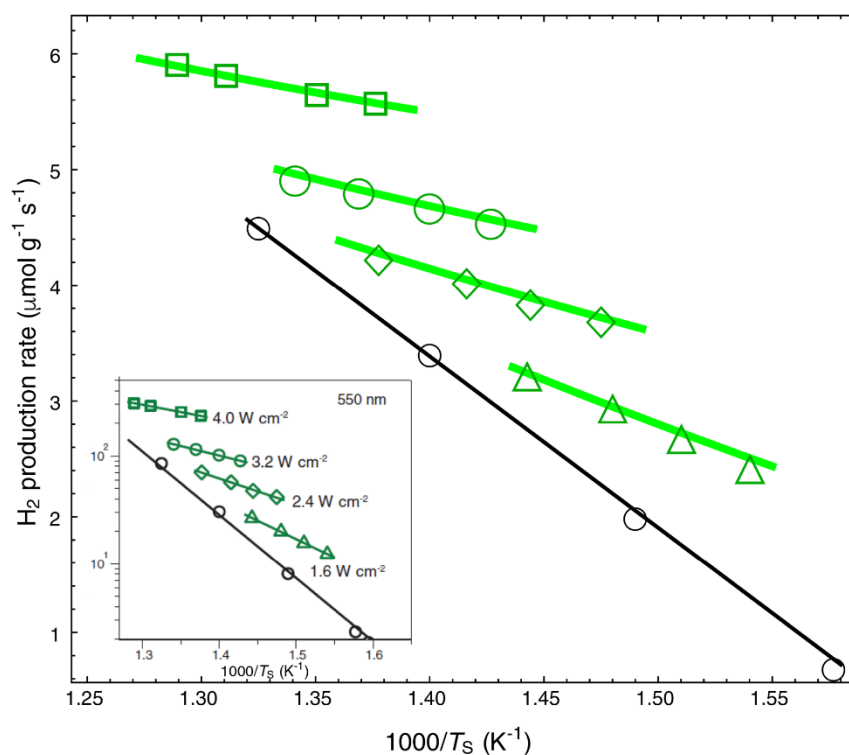


**Fig. 1. Reaction rates under different illumination intensities as a function of inverse (average measured) temperature.** The points correspond to the experimental data of (1). The solid lines are a fit to Eq. 2. The parameters (activation energy  $E_a$  and photothermal conversion coefficient  $a$ ) are extracted from the circles (in the dark) and the green squares (average intensity of 4 W/cm<sup>2</sup>). The curves for the rest of the datasets (green triangles, diamonds, circles) are obtained without additional fit parameters. Inset: Original data from (1).

## Comment on "Quantifying hot carrier and thermal contributions in plasmonic photocatalysis"

Yonatan Sivan, Joshua Baraban, Ieng Wai Un and Yonatan Dubi

*Science* **364** (6439), eaaw9367.  
DOI: 10.1126/science.aaw9367

ARTICLE TOOLS	<a href="http://science.sciencemag.org/content/364/6439/eaaw9367">http://science.sciencemag.org/content/364/6439/eaaw9367</a>
RELATED CONTENT	<a href="http://science.sciencemag.org/content/sci/364/6439/eaaw9545.full">http://science.sciencemag.org/content/sci/364/6439/eaaw9545.full</a> <a href="http://science.sciencemag.org/content/sci/362/6410/69.full">http://science.sciencemag.org/content/sci/362/6410/69.full</a>
REFERENCES	This article cites 13 articles, 1 of which you can access for free <a href="http://science.sciencemag.org/content/364/6439/eaaw9367#BIBL">http://science.sciencemag.org/content/364/6439/eaaw9367#BIBL</a>
PERMISSIONS	<a href="http://www.sciencemag.org/help/reprints-and-permissions">http://www.sciencemag.org/help/reprints-and-permissions</a>

Use of this article is subject to the [Terms of Service](#)